

Uplink Capacity in a CDMA Macrocell with a Hotspot Microcell: Exact and Approximate Analyses

Shalinee Kishore^{1,2}, Larry Greenstein², H. Vincent Poor¹, Stuart Schwartz¹

September 24, 2001

¹ Department of Electrical Engineering Princeton University Princeton, NJ 08544 U.S.A.	² Wireless Systems Research AT&T Labs - Research Middletown, NJ 07748 U.S.A.
--	--

Abstract

This paper studies the number of voice users (user capacity) supported on the uplink of a single-macrocell/single-microcell CDMA system. A “hotspot” microcell is embedded within a larger macrocell and operates over the same bandwidth as the larger cell. Analytic methods are presented for computing user capacity which account for propagation loss, multiple-access interference, power-control and random locations of user terminals, as well as two distinct methods by which users select base stations (tiers). Along with the *exact* user capacity, a technique for making accurate approximations is also presented. Simulation results verify both the exact and approximate analytical methods. This simulation is also employed to study the capacity gains of a third, more optimal, tier-selection scheme. These results point to differences in capacity performance based on the tier-selection method as well as on the traffic density within the hotspot region.

1 Introduction

Achieving high capacity is a principal aim of wireless operators, who often encounter small regions of high demand within a larger cell coverage area. Hotspot microcells comprise one architectural solution to these situations. Our aim here is to study the enhancements offered by a single code division multiple access (CDMA) hotspot microcell embedded within a single CDMA macrocell. We assume both

the macrocell and microcell operate over the same radio frequency channel. The key challenge here is to incorporate the effects of propagation loss, multiple-access interference, power control, random user locations, and the various methods by which users select base stations (tiers) in quantifying the number of users supported (i.e., the user capacity) on the uplink. The numerical results provide valuable insights into the performance of such systems.

Whether it is the uplink or downlink that limits capacity depends on many factors, including the radio techniques, propagation conditions and system architecture. Both directions bear examination but require different methods of analysis. In this paper, we develop a method for the uplink and use it to obtain results for that case.

The CDMA hotspot architecture was first examined in [1] which provides the foundation for understanding such systems. To facilitate analysis of this complex problem, Shapira assumed no shadow fading, simplified the treatment of user location distribution, and considered only one method of tier-selection (i.e., method by which users select which base station to communicate with). Subsequent papers, e.g., [2]-[15], that consider any of these aspects use analytical simplifications or resort solely to simulation. In [2], for example, the authors presented some analysis that considered lognormal shadowing, but then characterized the cross-tier interference via its mean value, which they computed using simulation. In [3], the authors demonstrated the benefits of power control in obtaining capacity gains on both the uplink and downlink. The results were, however, determined from simulation trials for a particular user location distribution and shadow fading was ignored. A study by Shin [4] illustrated the benefits of adapting tier-selection to user traffic. The results were based solely on simulations which also ignored shadow fading.

Building on these and other previous studies, e.g., [5]-[15], this paper contributes an exact analysis of uplink user capacity which includes (1) a general user location distribution; (2) full treatment of shadow fading; and (3) various distinct methods of tier-selection. The random nature of user location and shadow fading requires that the resulting user capacity be formulated in probabilistic terms, i.e., we compute the probability of achieving or exceeding a particular capacity. Capacity is studied as a function of both the number of users supported in the macrocell (N_M) and microcell (N_μ), and the total number of users in the system ($N = N_M + N_\mu$), where we mean the maximum number of users supported without call blocking. Due to the computational intensity of the exact analysis, a simple approximation method is desirable. We present one here and demonstrate its accuracy.

The exact and approximate analyses derive the uplink capacity for two classes of tier-selection schemes.

In the first class, a user selects a base according to the transmission losses between itself and the serving bases; the second class further accounts for the number of users being supported by each base. In addition, we also study the capacity gains of a third tier-selection method in which users decide between tiers based on the transmit power requirements. Due to the complexity of analyzing this last scheme, its capacity gains are studied here via simulation alone.

In Section 2, we detail the single-macrocell/single-microcell system treated here and also present the three tier-selection methods of interest. In Section 3, we present the analytical procedures with which to quantify capacity, and then propose a simple approximation. Section 4 begins with a description of an sample single-macrocell/single-microcell system. We then utilize our analysis as well as simulation techniques to study its performance. These results highlight the impact of the tier-selection method and the user location distribution. In Section 5 we summarize our findings and present ideas for future work.

2 System Description

2.1 Single Macrocell/Single Microcell Geometry

In the system studied here we are given a region of space \mathcal{R} over which the distribution of user terminals is known. We are also given that a macrocell base station of antenna height h_M and a microcell base station of antenna height h_μ are installed within the region \mathcal{R} . We utilize Cartesian coordinates (x, y) to describe locations in this region. The macrocell base station is placed at the origin and the microcell base station is a distance D from it, as shown in Figure 1. We assume the coordinate axes are chosen such that the microcell lies at the point $(D, 0)$. In terms of this coordinate system, the given distribution of user location is represented by $f_{XY}(x, y)$, where $(x, y) \in \mathcal{R}$. Observe that $f_{XY}(x, y) dx dy$ is the probability that a given user is in a small rectangle of area $dx dy$ centered at (x, y) .

The region \mathcal{R} contains N_M macrocell and N_μ microcell users, all transmitting at rate R on the uplink. The users have random codes of length W/R , where W is the system bandwidth. The two base stations employ matched filter receivers to detect the received bits and they control the transmit power of their users so that 1) the powers received from all of their users are equal, and 2) the signal-to-interference-plus-noise ratio (SINR) of all supported users meets a minimum requirement of Γ_M and Γ_μ at the macrocell and microcell, respectively.

Consistent with published propagation models, e.g., [16], we assume that a signal transmitted at power

P_t is received with mean power P_r according to

$$P_r = \begin{cases} P_t H \left(\frac{b}{d}\right)^2 10^{\zeta/10} & d < b \\ P_t H \left(\frac{b}{d}\right)^4 10^{\zeta/10} & d \geq b \end{cases} \quad (1)$$

where

- d is the distance between the transmitter and receiver antennas.
- b is “breakpoint” distance, where the slope of the decibel path gain changes. We refer to locations with $d < b$ as being inside the “breakpoint region.” The breakpoint distances for the macrocell and microcell are b_M and b_μ , respectively. Empirical data in [16] supports setting $b_M = b_\mu = 100$ m, which we will assume in our numerical calculations in Section 4. For analysis purposes, however, we assume general values of b_M and b_μ .
- H is a proportionality constant that depends on wavelength, antenna heights, antenna gains, etc. H_M and H_μ are the values of this constant for the macrocell and microcell, respectively. We assume $H_\mu \leq H_M$.
- ζ is a zero-mean normal random variable with standard deviation σ_M and σ_μ at the macrocell and microcell, respectively. The factor $10^{\zeta/10}$ represents the lognormal attenuation of the transmitted signal due to shadowing.

In addition to transmission loss, the transmitted signal is also impaired by receiver noise. This is modeled as additive white Gaussian noise (AWGN) whose power spectral density is η , assumed here to be the same at both bases.

We assume also that user terminals (handsets) do not have maximum transmit power constraints. Constraints on the transmit power are a realistic feature in all wireless systems. The assumption here implies scenarios with small macrocells and microcells, where users may never have to transmit at maximum power to communicate with the serving base station. For example, we observed in our simulations that cells of diameter 1 km require, for all users, maximum transmit powers less than 10 mW. This is well below the limit (1 mW) for current handsets.

2.2 Tier-Selection Methods

Both the macrocell and microcell base stations transmit a pilot signal. Each user in \mathcal{R} measures the received powers of the two pilots and elects to communicate with the base station with the stronger

signal. The strength of the transmitted pilot signal is in turn determined by the tier-selection method. In this paper we consider the following three tier-selection schemes:

1. T-based: The transmit power of the pilot signal is the same for both base stations. Each user consequently selects the base station with which it has a stronger transmission gain.
2. N-based: The transmit power of the pilot is reduced linearly with each serviced user. Users therefore tend to select the base station with the smaller number of users.
3. S-based: The pilot power varies as the reciprocal of the required received power at the base station. The user thus selects the base station with the minimum required transmit power.

Observe that the T-based method is a static tier-selection scheme. Once a user determines the base station with which to communicate, this selection does not change as the system load changes. The other two schemes are, on the other hand, dynamic selection methods; as users enter and exit the system the pilot strength changes, thereby requiring all users to readjust their tier selections.

2.3 Desensitivity and Pilot Powers

To achieve a desired microcell coverage, the microcell may have to be *desensitized*. Desensitization essentially means that the microcell raises its received power requirements to discourage outlying users from communicating with it. Implementationally, this means that the maximum transmit power of the microcell pilot, $P_{T\mu}$, is lowered below that of the macrocell, P_{TM} . We call $\delta = P_{T\mu}/P_{TM}$ the desensitivity of the microcell. Note that $\delta < 1$, and that smaller values of δ generally correspond to smaller microcell coverage areas. In the analysis below, we will show a simple way to incorporate desensitivity into the capacity study.

Depending on the tier-selection scheme, either base station may decide to transmit only a portion of the maximum pilot power. We denote the fraction of the maximum pilot power transmitted at the microcell and macrocell base station by f_μ and f_M , respectively. Thus the transmit powers of the pilots at the macrocell base and microcell base are $f_M P_{TM}$ and $f_\mu P_{T\mu}$, respectively. In the T-based scheme, $f_M = f_\mu$ and in the N-based scheme, $f_M = 1/N_M$ and $f_\mu = 1/N_\mu$. Finally in the S-based scheme, $f_M = 1/S_M$ and $f_\mu = 1/S_\mu$, where S_M and S_μ are the required received powers at the macrocell and microcell, respectively.

2.4 Performance Metrics

We wish to quantify the performance of the system described above and choose the following criterion: Given $f_{XY}(x, y)$, the location of the macrocell and microcell bases, the transmission loss model in (1),

and other system parameters (such as W , R , and η), what is the maximum number of users that can be supported in the uplink without call blocking?

We can compute this capacity in two ways. First, we may examine the user capacities in the two tiers, i.e. N_M and N_μ . On the other hand, we can compute total capacity, i.e. $N = N_M + N_\mu$. Due to random user locations and lognormal shadowing, user capacity – using either of these two definitions – must itself be examined in probabilistic terms (as further explained in Section 3). Let α be the probability, taken over all user positions and shadow fadings, that N_M macrocell users and N_μ microcell users can be supported simultaneously. We call α the *availability* for that combination of users, and we seek the $N_M - N_\mu$ contour below which $\alpha > \alpha_{cap}$, where α_{cap} is the *desired* value of availability (a typical value is $\alpha_{cap} = 0.95$). We will also find the value of *total* capacity, $N = N_M + N_\mu$, for which $\alpha > \alpha_{cap}$.

3 Methodology

3.1 Exact Capacity Analysis

3.1.1 Basic Equations

We begin our capacity analysis of the single-macrocell/single-microcell system with the uplink SINR equations. From these equations, we can determine required received power levels at the two bases. The uplink SINR values at the macrocell and microcell are, respectively,

$$(SINR)_M = \frac{S_M \frac{W}{R}}{\eta W + (N_M - 1)S_M + S_\mu \sum_{k \in \mu} \frac{T_{Mk}}{T_{\mu k}}} \quad (2)$$

$$(SINR)_\mu = \frac{S_\mu \frac{W}{R}}{\eta W + (N_\mu - 1)S_\mu + S_M \sum_{k \in M} \frac{T_{\mu k}}{T_{Mk}}} \quad (3)$$

where T_{jk} represents the transmission loss between user k and base j and M and μ are the sets of macrocell and microcell users, respectively. To meet the minimum SINR requirements, we set the above SINR values equal to Γ_M and Γ_μ and solve for the required S_M and S_μ :

$$S_M = \eta W \frac{(K_\mu - N_\mu) + \sum_{k \in \mu} \frac{T_{Mk}}{T_{\mu k}}}{(K_M - N_M)(K_\mu - N_\mu) - \sum_{k \in \mu} \frac{T_{Mk}}{T_{\mu k}} \sum_{k \in M} \frac{T_{\mu k}}{T_{Mk}}} \quad (4)$$

$$S_\mu = \eta W \frac{(K_M - N_M) + \sum_{k \in M} \frac{T_{\mu k}}{T_{Mk}}}{(K_M - N_M)(K_\mu - N_\mu) - \sum_{k \in \mu} \frac{T_{Mk}}{T_{\mu k}} \sum_{k \in M} \frac{T_{\mu k}}{T_{Mk}}} \quad (5)$$

where $K_j = \frac{W}{R\Gamma_j} + 1$. Note that K_j represents the single-cell *pole* capacity of cell j , i.e. the capacity in the absence of noise and other-cell interference. K_j , therefore, represents the maximum achievable

capacity for cell j .

To assess system capacity, we need to determine the combinations of N_M and N_μ for which the power control solutions above are feasible. Without constraints on transmit power, the solutions S_μ and S_M are feasible as long as they are non-negative. From (4) and (5), we see that S_μ and S_M are negative if and only if the identical denominator in (4) and (5) becomes negative. This denominator is itself a random variable that depends on the random locations and shadowings of the active users. Thus, as indicated earlier, we must look at capacity in probabilistic terms. More specifically, these two sources of randomness appear in the following normalized cross-tier interference terms:

$$I_\mu = \sum_{k \in M} \frac{T_{\mu k}}{T_{Mk}} \quad (6)$$

$$I_M = \sum_{k \in \mu} \frac{T_{Mk}}{T_{\mu k}} \quad (7)$$

$S_M I_\mu$ is the net interference measured at the microcell base due to active macrocell users. Similarly, $S_\mu I_M$ is the total interference at the macrocell base caused by microcell users. With the distributions of these two sums, the probability of a feasible solution can be computed for a given pair (N_M, N_μ) or for the sum, N . The computations of these two distributions are outlined below.

3.1.2 Probability Density Function (PDF) of I_M

The propagation model described earlier allows us to write I_M as

$$I_M = \sum_{k \in \mu} \frac{(x_k^2 + y_k^2 + D^2 + (h'_\mu)^2 - 2Dx_k)^{\gamma_{\mu k}}}{(x_k^2 + y_k^2 + (h'_M)^2)^{\gamma_{Mk}}} \frac{G_{Mk}}{G_{\mu k}} \frac{10^{\zeta_{Mk}/10}}{10^{\zeta_{\mu k}/10}} \equiv \sum_{k \in \mu} V_{M,k} \quad (8)$$

where:

- $h'_M = h_M - h_m$ and $h'_\mu = h_\mu - h_m$, with h_m the height of the antenna at the user terminal.
- x_k and y_k are random variables that describe the x and y coordinates of user k . Let $z_k = x_k^2 + y_k^2 + (h'_M)^2$ and $w_k = x_k^2 + y_k^2 + D^2 + (h'_\mu)^2 - 2Dx_k$. The random variable z_k represents the squared-distance between user k 's terminal antenna and the macrocell base antenna. Similarly, w_k represents the squared-distance between user k 's antenna and the microcell base antenna.
- The values γ_{Mk} , $\gamma_{\mu k}$, G_{Mk} , and $G_{\mu k}$ for each user k are specified based on the values of z_k and w_k :

$$\gamma_{Mk} = \begin{cases} 1, & z_k < b_M^2 \\ 2, & z_k \geq b_M^2 \end{cases} \quad (9)$$

$$\gamma_{\mu k} = \begin{cases} 1, & w_k < b_\mu^2 \\ 2, & w_k \geq b_\mu^2 \end{cases} \quad (10)$$

$$G_{Mk} = \begin{cases} H_M (b_M)^2, & z_k < b_M^2 \\ H_M (b_M)^4, & z_k \geq b_M^2 \end{cases} \quad (11)$$

$$G_{\mu k} = \begin{cases} H_\mu (b_\mu)^2, & w_k < b_\mu^2 \\ H_\mu (b_\mu)^4, & w_k \geq b_\mu^2 \end{cases} \quad (12)$$

- $10^{\zeta_{Mk}/10}$ is the lognormal attenuation of user k 's transmitted signal at the macrocell base due to shadowing. Similarly, $10^{\zeta_{\mu k}/10}$ is its attenuation at the microcell base. For simplicity, we denote $\chi_k = (10^{\zeta_{Mk}/10})/(10^{\zeta_{\mu k}/10})$. Since χ_k is the ratio of two lognormal random variables, it too is lognormal with $\sigma = \sqrt{\sigma_\mu^2 + \sigma_M^2}$. (We assume independence between $\zeta_{\mu k}$ and ζ_{Mk} and that χ_k is independent of z_k and w_k .)

Note that I_M is a sum of *independent identically-distributed* (iid) random variables. Thus, to compute its distribution, we begin by deriving the probability density function (PDF) of any one term in the sum, and then use N_μ -fold convolution.

According to the propagation model, the single-macrocell/single-microcell system may be composed of four disjoint propagation regions¹:

- **Region 1:** $R_1 = \{(z, w) | z \in (b_M^2, z_{\max}], w \in (b_\mu^2, w_{\max}]\}$
- **Region 2:** $R_2 = \{(z, w) | z \in [z_{\min}, b_M^2], w \in (b_\mu^2, w_{\max}]\}$
- **Region 3:** $R_3 = \{(z, w) | z \in [z_{\min}, b_M^2], w \in [w_{\min}, b_\mu^2]\}$
- **Region 4:** $R_4 = \{(z, w) | z \in (b_M^2, z_{\max}], w \in [w_{\min}, b_\mu^2]\}$

where z_{\max} and w_{\max} are the maximum values that z and w can take on, and $z_{\min} = (h'_M)^2$ and $w_{\min} = (h'_\mu)^2$. Depending on D , b_M , and b_μ , some or all of these regions may exist over the terrain. An example of these four regions is shown in Figure 2 over a square region \mathcal{R} .

In order to describe the distribution I_M , we need to first establish the joint distribution of z and w , i.e. the squared-distance terms described earlier. To compute this joint distribution, $f_{ZW}(z, w)$, we

¹For simplicity we drop the index k

will make use of the given distribution $f_{XY}(x, y)$. It can be shown using the Jacobian [17], that

$$f_{ZW}(z, w) = g(z, w) \cdot f_{XY} \left(\frac{z + D^2 - w + (h'_\mu)^2 - (h'_M)^2}{2D}, \frac{1}{4Dg(z, w)} \right) + g(z, w) \cdot f_{XY} \left(\frac{z + D^2 - w + (h'_\mu)^2 - (h'_M)^2}{2D}, -\frac{1}{4Dg(z, w)} \right)$$

where

$$g(z, w) = \frac{1}{4D \sqrt{z - (h'_M)^2 - \left(\frac{z + D^2 - w + (h'_\mu)^2 - (h'_M)^2}{2D} \right)^2}}$$

We now summarize how to compute the distribution of I_M :

1. As implied by (8), V_M is a random variable that represents each term in the sum I_M . Observe that V_M is the ratio of the random transmission loss between a *microcell* user and the macrocell base to the transmission loss between this user and the microcell base. If the tier-selection method employed is strictly T-based (without desensitivity), then $V_M \leq 1$. With a desensitivity of δ , $V_M \leq \delta$. For the N-based scheme without desensitivity, $V_M \leq N_M/N_\mu$, and so on. In our analysis we simply require that $V_M \in [0, v_{\max}]$, where v_{\max} can be determined from tier-selection method and the desensitivity.
2. We begin by computing the cumulative distribution function (CDF) of V_M , $F_{V_M}(v)$. To facilitate this, we first condition on the random variable χ ; that is, we start by computing $F_{V_M|\chi}(v|\chi)$.
3. If the interfering microcell user lies in Region 1, then its contribution to the cross-tier interference at the macrocell is $V_M = \chi \frac{W^2}{Z^2} \cdot \frac{H_M b_M^4}{H_\mu b_\mu^4}$. On the other hand, if the user is in Region 2, $V_M = \chi \frac{W^2}{Z} \cdot \frac{H_M b_M^2}{H_\mu b_\mu^4}$, and so on. The CDF of V_M is

$$F_{V_M|\chi}(v|\chi) = \mathbb{P}[V_M \leq v | V_M \leq v_{\max}, \chi] \quad (13)$$

$$= \sum_{i=1}^4 \mathbb{P}[V_M \leq v | V_M \leq v_{\max}, R_i, \chi] \cdot \mathbb{P}[R_i] \quad (14)$$

Observe that,

$$\mathbb{P}[R_1] = \mathbb{P}[\text{Region 1}] = \int_{b_\mu^2}^{w_{\max}} \int_{b_M^2}^{z_{\max}} f_{ZW}(z, w) dz dw \quad (15)$$

$$\mathbb{P}[R_2] = \mathbb{P}[\text{Region 2}] = \int_{b_\mu^2}^{w_{\max}} \int_{z_{\min}}^{b_M^2} f_{ZW}(z, w) dz dw \quad (16)$$

$$\mathbb{P}[R_3] = \mathbb{P}[\text{Region 3}] = \int_{w_{\min}}^{b_\mu^2} \int_{z_{\min}}^{b_M^2} f_{ZW}(z, w) dz dw \quad (17)$$

$$\mathbb{P}[R_4] = \mathbb{P}[\text{Region 4}] = \int_{w_{\min}}^{b_\mu^2} \int_{b_M^2}^{z_{\max}} f_{ZW}(z, w) dz dw \quad (18)$$

and

$$\mathbb{P}[V_M \leq v | V_M \leq v_{\max}, R_i, \chi] = \frac{\mathbb{P}[V_M \leq v, V_M \leq v_{\max}, R_i | \chi]}{\mathbb{P}[V_M \leq v_{\max}, R_i | \chi]}$$

where $i = 1, 2, 3, 4$.

4. In Region 1, $V_M = \beta \chi \frac{Z^2}{W^2}$, where $\beta = \frac{H_M b_M^4}{H_\mu b_\mu^4}$, we have

$$\begin{aligned} & \mathbb{P}[V_M \leq v, V_M \leq v_{\max}, R_1 | \chi] \\ &= \mathbb{P}[Z \leq \sqrt{\frac{v}{\beta \chi}} W, Z \leq \sqrt{\frac{v_{\max}}{\beta \chi}} W, Z > b_M^2, W > b_\mu^2] \\ &= \int_{b_M^2}^{\max(b_M^2, \min(z_{\max}, \sqrt{\frac{v'}{\beta \chi}} w_{\max}))} \int_{\min(w_{\max}, \max(b_\mu^2, z \sqrt{\frac{\beta \chi}{v'}}))}^{w_{\max}} f_{ZW}(z, w) dw dz \end{aligned}$$

where

$$v' = \begin{cases} v, & v \leq v_{\max} \\ v_{\max}, & \text{otherwise} \end{cases}$$

Also note that

$$\begin{aligned} & \mathbb{P}[V_M \leq v_{\max}, R_1 | \chi] \\ &= \int_{b_M^2}^{\max(b_M^2, \min(z_{\max}, \sqrt{\frac{v_{\max}}{\beta \chi}} w_{\max}))} \int_{\min(w_{\max}, \max(b_\mu^2, z \sqrt{\frac{\beta \chi}{v_{\max}}}))}^{w_{\max}} f_{ZW}(z, w) dw dz \end{aligned}$$

5. We can compute the CDF of V_M in each of the other three regions in the same manner. For the sake of brevity, we do not include those results here. After computing these conditional CDF's over the four propagation regions, we combine them as indicated in (14) to obtain $F_{V_M|\chi}(v|\chi)$.
6. Thus far we have determined the CDF of V_M given the shadowing random variable. The unconditional CDF can be computed as:

$$F_{V_M}(v) = \begin{cases} 0, & v \leq 0 \\ \int_0^\infty F_{V_M|\chi}(v|\chi) \cdot f_\chi(\chi) d\chi, & v \in [0, v_{\max}] \\ 1, & v > v_{\max} \end{cases}$$

where $f_\chi(\chi)$ is a lognormal PDF with $\sigma = \sqrt{\sigma_M^2 + \sigma_\mu^2}$.

7. The PDF of V_M is then

$$f_{V_M}(v) = \begin{cases} \frac{dF_{V_M}(v)}{dv}, & v \in [0, v_{\max}] \\ 0, & \text{otherwise} \end{cases} \quad (19)$$

8. Since I_M is the sum of N_μ iid random variables with distribution $f_{V_M}(v)$, we compute the PDF of I_M by taking the N_μ -fold convolution of the individual PDF's.

3.1.3 Probability Density Function of I_μ

Using the propagation model described earlier, we can write I_μ as:

$$I_\mu = \sum_{k \in M} \frac{(x_k^2 + y_k^2 + (h'_M)^2)^{\gamma_{Mk}}}{(x_k^2 + y_k^2 + D^2 + (h'_\mu)^2 - 2Dx_k)^{\gamma_{\mu k}}} \frac{G_{\mu k}}{G_{Mk}} \frac{10^{\zeta_{\mu k}/10}}{10^{\zeta_{Mk}/10}} \equiv \sum_{k \in M} V_{\mu, k} \quad (20)$$

In a similar manner, we first derive the PDF of a term in the sum. V_μ is a random variable that describes each term in the sum I_μ . We wish to compute the PDF (via the CDF) of V_μ given $V_\mu \leq \frac{1}{v_{\max}}$. We do this using the steps employed in computing the distribution of V_M . Once again, for brevity we do not include these results; and, similar to the case for I_M , we compute I_μ via a N_M -fold convolution. This is not detailed here, as it follows the derivation of the distribution of I_M .

3.1.4 Infeasibility of Power Control Solution

As stated earlier, the power control solution described in (4) and (5) is infeasible if the identical denominator term is negative. For a given value of N_M and N_μ , we can therefore compute the probability of an infeasible solution as

$$P_{\text{inf}}(N_M, N_\mu) = \text{P}[I_M I_\mu > (K_M - N_M)(K_\mu - N_\mu)] \quad (21)$$

Now, observe that I_M and I_μ are independent random variables that are bounded: $I_M \in [0, N_M v_{\max}]$ and $I_\mu \in [0, \frac{N_M}{v_{\max}}]$. Let $Y = I_M I_\mu$. The CDF of Y can be computed as

$$\text{P}[Y \leq y] = \text{P}[I_M I_\mu \leq y] \quad (22)$$

$$= \text{P}[I_\mu \leq y/I_M] \quad (23)$$

$$= \int_0^{\frac{N_M}{v_{\max}}} \int_0^{\min(\frac{y}{i_\mu}, N_\mu v_{\max})} f_{I_\mu}(i_\mu) f_{I_M}(i_M) di_M di_\mu \quad (24)$$

The probability of an infeasible power control solution is then:

$$P_{\text{inf}}(N_M, N_\mu) = 1 - \text{P}[Y \leq (K_M - N_M)(K_\mu - N_\mu)]$$

We can now compute system capacity based on the infeasibility of the power control equation. Suppose we want to have feasible power control solutions at least 95% of the time, i.e. $\alpha_{cap} = 0.95$. To do so, we first solve for Y such that $P_{\text{inf}}(N_M, N_\mu) = 0.05$, then equate it to $(K_M - N_M)(K_\mu - N_\mu)$, and finally solve for N_M given N_μ .

We can also look at capacity as the *total* number of users supported by the system. Assume that we are given N total users. Out of N , there are N_μ microcell users and $N - N_\mu$ macrocell users.

Given N and N_μ , the probability of an infeasible solution, $P_{\text{inf}}(N - N_\mu, N_\mu)$, can be computed using the results given earlier. Now the probability that given N users N_μ will be microcell users can be calculated by first computing the probability that any one user in the system is a microcell user:

$$p = \text{P}[1 \text{ microcell user}] \quad (25)$$

$$= \sum_{i=1}^4 \text{P}[1 \text{ microcell user in } R_i] \cdot \text{P}[R_i] \quad (26)$$

Note,

$$\text{P}[1 \text{ microcell user in } R_i] = \text{P}[V_M \leq v_{\text{max}}, R_i]$$

Observe that we have already shown how to compute this. With N total users, the probability of n microcell users is then

$$\text{P}[N_\mu = n|N] = \binom{N}{n} p^n (1-p)^{(N-n)} \quad (27)$$

Therefore, we see that, that the probability of an infeasible solution given N is

$$P_{\text{inf}}(N) = \sum_{n=0}^N \binom{N}{n} p^n (1-p)^{(N-n)} P_{\text{inf}}(N-n, n) \quad (28)$$

We can calculate the above probability for varying values of N . For example, if we determine the N value that corresponds to 95% feasibility (5% infeasibility), we can say that this is the capacity achievable 95% of the time.

3.2 Approximating Capacity

We showed above that the power control solutions become infeasible when $I_\mu I_M > (K_\mu - N_\mu)(K_M - N_M)$. Since both I_μ and I_M are random variables, the resulting system capacity is also a random variable, as described above. We now approximate system capacity by utilizing the means of I_μ and I_M .

Let V_M and V_μ be the iid terms in the summations I_M and I_μ , respectively, where $V_M \leq v_{\text{max}}$ and $V_\mu \leq \frac{1}{v_{\text{max}}}$. Clearly, the mean of I_μ is N_M times the mean of V_μ , and similarly the mean of I_M is N_μ times the mean of V_M . Therefore, we can then approximate capacity as all pairs (N_μ, N_M) such that

$$\text{E}[V_\mu | V_\mu \leq \frac{1}{v_{\text{max}}}] \text{E}[V_M | V_M \leq v_{\text{max}}] = \bar{V}_M \bar{V}_\mu \leq \frac{(K_\mu - N_\mu)(K_M - N_M)}{N_\mu N_M} \quad (29)$$

The $N_\mu - N_M$ contour implied by this relationship is

$$N_\mu = \frac{K_\mu(K_M - N_M)}{K_M - N_M(1 - \bar{V}_M \bar{V}_\mu)} \quad (30)$$

Observe that (30) can be modified as

$$n_\mu = \frac{(1 - n_M)}{1 - n_M(1 - \bar{V}_M \bar{V}_\mu)} \quad (31)$$

where $n_M = \frac{N_M}{K_M}$ and $n_\mu = \frac{N_\mu}{K_\mu}$. The contour in (31) depends solely on \bar{V}_M and \bar{V}_μ which, as we will see depends on the distribution of users, propagation model, tier-selection method, and desensitivity. It is entirely independent of such system parameters as W , R , Γ_M , and Γ_μ and thus applies generally to any second- or third-generation CDMA system.

To compute the contours (30) and (31), we must determine \bar{V}_μ and \bar{V}_M . Starting first with \bar{V}_M , we note that

$$V_M = \frac{\chi}{r(z, w)} \leq v_{\max} \quad (32)$$

where χ is as described earlier, and

$$r(z, w) = \frac{z^{\gamma_M} G_\mu}{w^{\gamma_\mu} G_M} \quad (33)$$

As previously noted, G_M , G_μ , γ_M , and γ_μ are propagation constants that depend on the propagation region, i.e. on the values of z and w . We may then write

$$\bar{V}_M = E[V_M | V_M \leq v_{\max}] = E_{(z,w)} [E_\chi[V_M | V_M \leq v_{\max} \& (z, w)] | (z, w)] \quad (34)$$

Now,

$$\begin{aligned} E_\chi[V_M | V_M \leq v_{\max} \& (z, w)] &= E_\chi \left[\frac{\chi}{r(z, w)} \mid \frac{\chi}{r(z, w)} \leq v_{\max} \& (z, w) \right] \\ &= \frac{1}{r(z, w)} E[\chi | \chi \leq v_{\max} r(z, w)] \end{aligned}$$

It can be shown that

$$E[\chi | \chi \leq v_{\max} r(z, w)] = \frac{e^{\sigma_o^2/2} \left(1 - Q \left(\frac{\ln v_{\max} r(z, w) - \sigma_o^2}{\sigma_o} \right) \right)}{1 - Q \left(\frac{\ln v_{\max} r(z, w)}{\sigma_o} \right)} \quad (35)$$

where $\sigma_o = \frac{\sigma \ln 10}{10}$, $\sigma = \sqrt{\sigma_M^2 + \sigma_\mu^2}$ (as before), and $Q(\cdot)$ is the complementary CDF of a normal random variable.

Observe that the form of $r(z, w)$ depends on the region of propagation. Therefore, we compute \bar{V}_M as

$$\bar{V}_M = \sum_{i=1}^4 \int \int_{R_i} f_{ZW}(z, w) \frac{1}{r_i(z, w)} E[\chi | \chi \leq v_{\max} r_i(z, w)] dw dz \quad (36)$$

where $r_1(z, w) = \frac{H_\mu b_\mu^4 z^2}{H_M b_M^4 w^2}$, $r_2(z, w) = \frac{H_\mu b_\mu^4 z}{H_M b_M^2 w^2}$, $r_3(z, w) = \frac{H_\mu b_\mu^2 z}{H_M b_M^2 w}$, and $r_4(z, w) = \frac{H_\mu b_\mu^2 z^2}{H_M b_M^4 w}$.

Similarly, we compute \bar{V}_μ by first noting

$$V_\mu = \chi \cdot r(z, w) \leq \frac{1}{v_{\max}} \quad (37)$$

Following the steps as we did to compute \bar{V}_M , we can show that

$$\bar{V}_\mu = \sum_{i=1}^4 \int \int_{R_i} f_{ZW}(z, w) r_i(z, w) \mathbb{E} \left[\chi | \chi \leq \frac{1}{v_{\max} r_i(z, w)} \right] dw dz \quad (38)$$

where

$$\mathbb{E} \left[\chi | \chi \leq \frac{1}{v_{\max} r_i(z, w)} \right] = \frac{e^{\sigma_o^2/2} \left(1 - Q \left(\frac{\ln \frac{1}{v_{\max} r_i(z, w)} - \sigma_o^2}{\sigma_o} \right) \right)}{1 - Q \left(\frac{\ln \frac{1}{v_{\max} r_i(z, w)}}{\sigma_o} \right)} \quad (39)$$

These mean calculations allow us to approximate capacity on the $N_M - N_\mu$ plane. The reliability of this method is examined in Section 4 and is shown to be excellent. An accurate approximation technique like this may help in studying the capacity of systems with multiple macrocells and microcells.

3.3 Modeling S-Based (Optimal) Tier-Selection

The previous two sections demonstrate analytical methods for the T-based and N-based selection schemes. We now focus on the S-based method. In this scheme, each user selects between the two base stations so as to minimize its transmit power. To this end, we present the following algorithm:

1. Initially, assign users based on transmission loss and compute S_μ and S_M .
2. For each user, determine the transmit power that meets requirement S_μ at the microcell and S_M at the macrocell.
3. If the required transmit power for a user is lower at the other tier, switch tiers and update the S_μ and S_M values.
4. Repeat 2 and 3 until convergence of S_M and S_μ .

In [18] and [19], the authors presented base selection algorithms for single-tier systems that minimized the total transmit power in the system (i.e., the sum over all uplink transmitters). Though algorithmically different, the S-based scheme and the schemes in [18] and [19] lead to the same base station assignments whenever a feasible solution exists. Feasibility, in this context, means that there exists a base station assignment such that the minimum SINR requirements can be met on all links. Moreover, as we observed in simulation trials, the S-based algorithm converges significantly faster than the other algorithms. However, these earlier schemes lead to feasible assignments at each step of the algorithm while the S-based algorithm may not necessarily do so. It may therefore be implementationally problematic; but it does, for our purposes, produce identical capacity results as the algorithms in [18] and [19] using a significantly faster simulation. Also note that the study here considers hard handoff between tiers. The implementation issue cited may not exist in systems with soft handoff, a subject worthy of further study.

4 Results

We now examine the performance of a particular single-macrocell/single-microcell system. We begin by postulating an example distribution $f_{XY}(x, y)$. We then present capacity results using both the analysis and simulation methods described above.

4.1 A Square Distribution of Users

We define a square region \mathcal{R} with side of length S as shown in Figure 3. As in Figure 1, we assume the macrocell base station is located at the center of this square and the microcell base is embedded at a point $(D, 0)$. We postulate two types of users in this system: (1) *low-density* (LD) users who are uniformly distributed over \mathcal{R} and (2) additional *high-density* (HD) users who are uniformly distributed in a smaller square region $(\mathcal{R}_{HD}, \mathcal{R}_{HD} \in \mathcal{R})$ around the microcell base. We assume the length of the side of the HD square region is s .² Also, we define P_h as the probability that a user in the general population is a HD user, and we call this the hotspot density. If $P_h = 0$, then there are only LD users in the system, uniformly distributed over the larger square region \mathcal{R} . If, on the other hand, $P_h = 1$, then there are only HD users in the system, uniformly distributed over the smaller square. For such a description, $f_{XY}(x, y)$ can be written as

$$f_{XY}(x, y) = \begin{cases} 1 - P_h + \frac{P_h}{s^2}, & (x, y) \in \mathcal{R}_{HD} \\ 1 - P_h, & (x, y) \in \mathcal{R} \setminus \mathcal{R}_{HD} \end{cases} \quad (40)$$

where,

$$\begin{aligned} \mathcal{R}_{HD} &= \left\{ (x, y) \mid x \in \left[D - \frac{s}{2}, D + \frac{s}{2} \right] \ \& \ y \in \left[-\frac{s}{2}, \frac{s}{2} \right] \right\} \\ \mathcal{R} &= \left\{ (x, y) \mid x \in \left[-\frac{1}{2}, \frac{1}{2} \right] \ \& \ y \in \left[-\frac{1}{2}, \frac{1}{2} \right] \right\} \end{aligned}$$

For this $f_{XY}(x, y)$, we can approximate total capacity N by first assuming that the probability that a given user is connected to the microcell is roughly equal to P_h , i.e. $p \approx P_h$. (Hotspot microcells are embedded in macrocells so as to provide coverage to a particular region, and we assume here that this region is essentially the location of the HD users.) We can then approximate total capacity as before (Section 3.1.4), except that we use P_h for p and replace (28) with

$$P_{\text{inf}}(N) \approx \sum_{n=0}^N \binom{N}{n} p^n (1-p)^{(N-n)} I(N-n, n) \quad (41)$$

²In our numerical calculation we assume $s = 2b_\mu$. This leads to a microcell design in which the HD users receive strong signals from the microcell base.

where

$$I(N_M, N_\mu) = \begin{cases} 1, & N_\mu N_M \geq \frac{(K_\mu - N_\mu)(K_M - N_M)}{V_M V_\mu} \\ 0, & \text{otherwise} \end{cases} \quad (42)$$

The selector function I comes from invoking (29). For this system, we compute the exact and approximate capacity analytically for the T-based scheme only. As stated earlier, the analysis can be used to evaluate the N-based scheme as well. However, the resulting capacity for this scheme (as well as for the S-based scheme) can be more quickly and easily obtained using simulation, and that is what we have done. The algorithm used in implementing this is similar to that of the S-based scheme described in Section 3.3.

4.2 Capacity Results

For the $f_{XY}(x, y)$ described above, we determine the values (N_M, N_μ) for which there are feasible solutions with probability 0.95. We assume – here as in all other results – the parameters listed in Table 1. To determine the (N_M, N_μ) values, we employ the analysis in Section 3 and simulation, assuming a T-based tier-selection method without desensitivity. In particular, we compute the distributions of (8) and (20) via numerical convolution, which we found to be more reliable than transform methods.

The first set of results is presented in Figure 4. Here we plot contours of feasible number of macrocell and microcell users for $P_h = 0.5$. The simulation and analysis results match closely. All pairs of N_M and N_μ inside the contour lead to feasible solutions with probability greater than 0.95. Included in Figure 4 is the contour obtained using the approximation method, demonstrating its accuracy. We have also included the median contour, i.e. the contour for $\alpha_{cap} = 0.5$. This curve indicates the spread of (N_M, N_μ) values is not large; for any N_M value the median curve indicates at most 2 more microcell users than the 95% curve. The shaded region in Figure 4 corresponds to the $\pm 2\sigma$ operating points, i.e. the N_M and N_μ values that occur within ± 2 standard deviations of the average N_M and N_μ values. The simulation points occur more frequently within this operating region and are therefore more reliable than those at the extremities of the contour.

We show the same set of results for $P_h = 0.875$ in Figure 5. Here, the operating region has shifted to produce larger N_μ values. This is because the hotspot region contains more users. As a first approximation, most of these hotspot users select the microcell base, thereby resulting in larger N_μ values. Here, too, we observe the close correspondence between the analytical and simulation results for those points in the operating region. Also, once again, the approximation serves as a reliable measure of capacity; and the median curve lies close to the 95% capacity contour.

We now examine the same distribution of users, but with the aim of determining total capacity, N . In Figure 6 we show total capacity as a function of P_h for the T-based tier-selection method. The simulation and analytical results are once again extremely close. The total capacity is largest around $P_h = 0.5$. As the hotspot density increases or decreases from this optimum region, the total capacity decreases. For reference, we have indicated the single-cell pole capacity K_M in Figure 6, as well as the capacity that would have resulted with two non-interfering cells, i.e., $K_M + K_\mu$. At the extremes of $P_h = 1$ or $P_h = 0$, the total capacity is essentially that of a single-cell system; the benefit of having two bases cannot be exploited. In the region of $P_h = 0.5$, the capacity increases 45% above that of a single-cell system and is roughly 30% below that of two non-interfering cells. We have also included in this figure the capacity computed using the approximation described above. We see that the approximate method here predicts capacity within 2 users for all values of P_h . The approximate capacity is in fact a pessimistic measure for low and high values of P_h and is extremely accurate in the mid-range.

In Figure 7, we show the same capacity results as in Figure 6 but, in addition, we plot the capacity for the S-based tier-selection method, as well as the T-based method with a desensitivity of $\delta = 0.5$ (3 dB). The plot indicates that the performance of the S-based scheme is almost invariant to the hotspot density. In the region of $P_h = 0.5$, the T-based scheme performs almost as well as the S-based scheme. The desensitized T-based scheme results in less total capacity for most values of P_h . This occurs because of the increased interference at the macrocell, which results in fewer supported users in the macrocell tier. Interestingly, the performance of the desensitized scheme outperforms the scheme without desensitivity for high values of P_h . In this range of P_h values, the increase in microcell users (due to larger values of P_h) exceeds the capacity hit taken at the macrocell due to the increased cross-tier interference.

Finally, we can look at system capacity using a slightly different simulation method. The results are presented in Figure 8. Here, we plot capacity contours in the $N_h - N_l$ plane, where N_h and N_l denote the number of HD and LD users, respectively. For a fixed number of N_l users, the simulation determined the N_h value supported over at least 0.95 of the trials. In the simulation, we employed all three tier-selection methods without desensitivity. We also implemented the T-based scheme with desensitivity of $\delta = 0.5$. The results show the superior capacity performance for the S-based scheme. The T-based scheme leads to the smallest capacity, while the N-based scheme operates in between. In the range near $N_l \approx N_h$ ($P_h \approx 0.5$), all three schemes perform roughly the same.

Using our simulation platform, we obtained other results. Rather than include multiple plots to show these secondary results, we simply state them: For a system with a circular LD region and a circular

HD region, where the areas are equal to the square LD and HD regions, we observe identical performance when compared to the square LD and HD results. We observed this for all three tier-selection methods. Additionally, the reverse experiment, i.e. determining the 95% value of N_l for a given value of N_h , produces the same capacity contours.

5 Conclusion

We have presented a general analytical framework with which to compute uplink user capacity for a single-macrocell/single-microcell CDMA system. Using simulations we showed the validity of the analytical method as well as the reliability of an alternative (and far simpler) approximate method. In contrast to previous work, our approach assumes a general user location distribution, incorporates lognormal shadowing, and examines three different tier-selection methods. The results help us quantify the differences in capacity for the various tier-selection methods as well as for varying degrees of hotspot density. Future work in this area should consider more complex architectures (i.e., with multiple macrocells and microcells) and also the effects of maximum transmit power constraints and soft-handoff. The analytical framework presented here should be useful in treating these cases.

References

- [1] J. Shapira. “Microcell Engineering in CDMA Cellular Networks,” *IEEE Transactions on Vehicular Technology*, Volume 43, No. 4, pp. 817–825, November, 1994.
- [2] J. J. Gaytán and D. Muñoz Rodríguez. “Analysis of Capacity Gain and BER Performance for CDMA Systems with Desensitized Embedded Microcells. International Conference on Universal Personal Communications (ICUPC 98), Volume 2, pp. 887–891, 1998.
- [3] J. S. Wu, et al. “Performance Study for a Microcell Hot Spot Embedded in CDMA Macrocell Systems,” *IEEE Transactions on Vehicular Technology*, Volume 48, No. 1, pp. 47–59, January, 1999.
- [4] S. H. Shin, et al. “Power Control and QOS of a CDMA based Hierarchical Cell Structure Network,” IEEE Region 10 Conference (TENCON 99), Volume 2, pp. 1220–1223, 1999.
- [5] S. Hämäläinen, et al. “Performance of a CDMA Based Hierarchical Cell Structure Network,” Personal, Indoor, and Mobile Radio Communications (PIMRC 97), Volume 3, pp. 863–866, 1997.
- [6] D. D. Lee, et al. “Other-Cell Interference with Power Control in Macro/Microcell CDMA Networks,” Vehicular Technology Conference (VTC 96), Volume 2, pp. 1120–1124, 1996.

- [7] J.Y. Kim, et al. “Macrodiversity Power Control in Hierarchical CDMA Cellular Systems,” Vehicular Technology Conference (VTC 99), Volume 4, pp. 2418–2422, Fall 1999.
- [8] I. Ghaleb, et al. “Tiered Services/Private System Support for CDMA Systems,” Vehicular Technology Conference (VTC 99), Volume 3, pp. 2260–2263, 1999.
- [9] J. S. Wu, et al. “Analysis of Uplink and Downlink Capacities for Two-tier Cellular System,” *IEE Proc.-Comm*, Volume 144, Issue 6, pp. 405–411, 1997.
- [10] J.S. Wu. “Performance Study of Multi-channel Access Schemes in Two-tier CDMA Cellular Systems,” Vehicular Technology Conference (VTC 98), Volume 3, pp. 2441–2445, 1998.
- [11] J. Yang and M. Rajan. “Microcell Performance Evaluation in IS-95 based CDMA Networks,” Volume 2, pp. 899–903, 1998.
- [12] J. Wang and L. B. Milstein. “Approximate Interference of a Microcellular Spread Spectrum System,” *Electronics Letters*, Volume 31, No. 20, pp. 1782–1783, September, 1995.
- [13] J. Castañeda-Camacho and D. Lara-Rodriguez. “Performance of a New Microcell/Macrocell Cellular Architecture with CDMA Access,” Vehicular Technology Conference (VTC 2000), Volume 1, pp. 483–486, Spring, 2000.
- [14] D. H. Kim, et al. “Capacity Analysis of Macro/Microcellular CDMA with Power Ratio Control and Tilted Antenna,” *IEEE Transactions on Vehicular Technology*, Volume 49, No. 1, pp. 34–42, January, 2000.
- [15] I. Bazar, et al. “Effects of Cell Distance on Capacity of Two-tier Cellular Networks,” International Conference on Universal Personal Communications (ICUPC 98), Volume 1, pp. 537–541, 1998.
- [16] V. Erceg, et al. “An Empirically based Path Loss Model for Wireless Channels in Suburban Environments. *IEEE Journal on Selected Areas in Communications*, Volume 17, No. 7, pp. 1205–1211, July, 1999.
- [17] A. Papoulis. *Probability, Random Variables, and Stochastic Processes*. McGraw-Hill, 1965.
- [18] R. Yates. “A Framework for Uplink Power Control in Cellular Radio Systems,” *IEEE Journal in Selected Areas in Communications*, Volume 13, No. 7, pp. 1341–1348, September, 1995.
- [19] S. V. Hanly. “An Algorithm for Combined Cell-Site Selection and Power Control to Maximize Cellular Spread Spectrum Capacity,” *IEEE Journal in Selected Areas in Communications*, Volume 13, No. 7, pp. 1332–1340, September, 1995.

W/R	128	h_m	1.5 m
Γ_M	7 dB	Γ_μ	7 dB
h_M	60 m	h_μ	9 m
b_M	100 m	b_μ	100 m
H_M	$10H_\mu$	D	300 m
σ_M	8 dB	σ_μ	4 dB
s	200 m	S	1 km

Table 1: System parameters used in Section 4

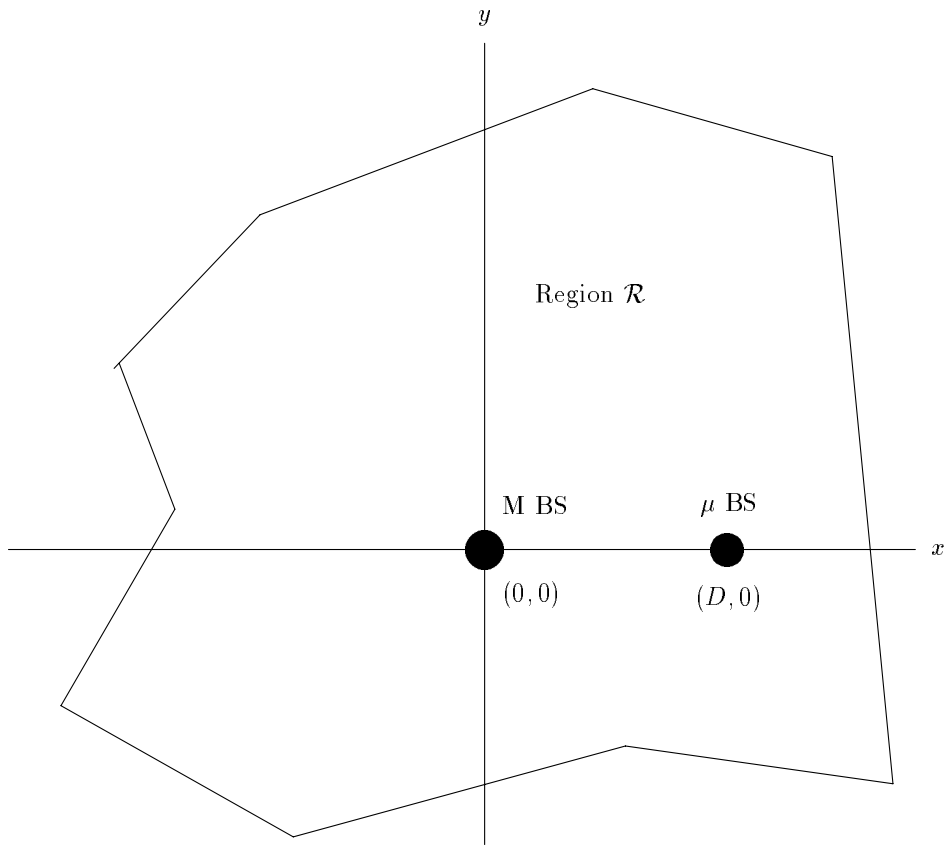


Figure 1: An example of a region \mathcal{R} , macrocell base station and microcell base station installation.

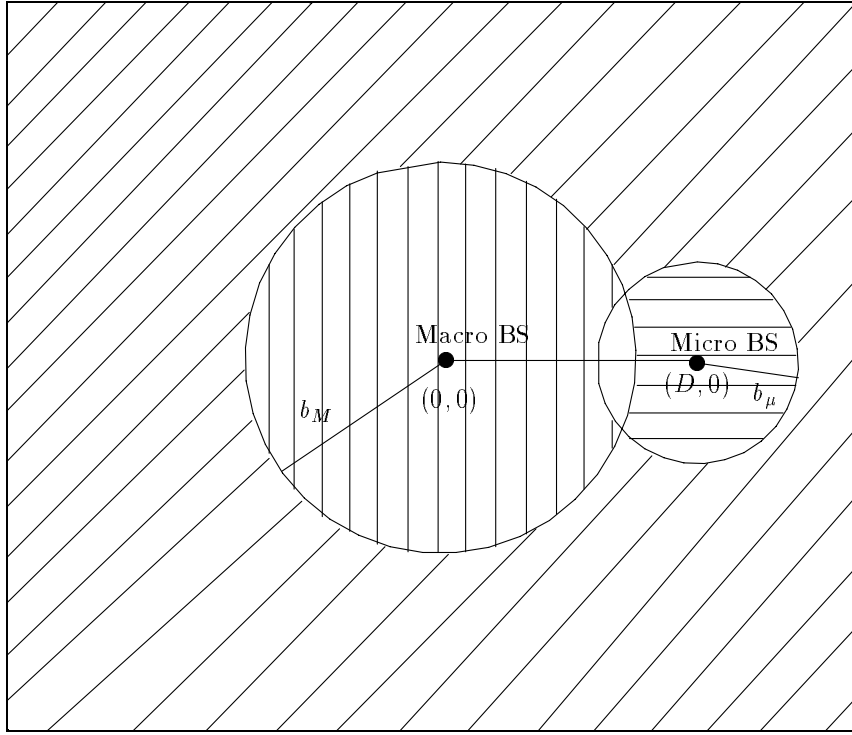


Figure 2: An example of a square region \mathcal{R} with the four propagation regions.

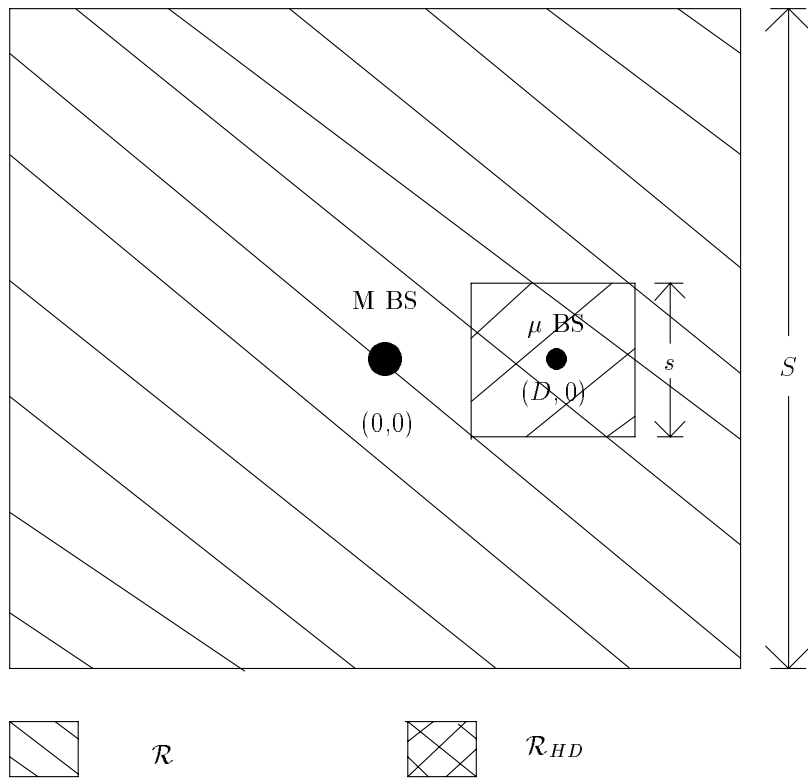


Figure 3: Description of $f_{XY}(x, y)$ used in Section 4.

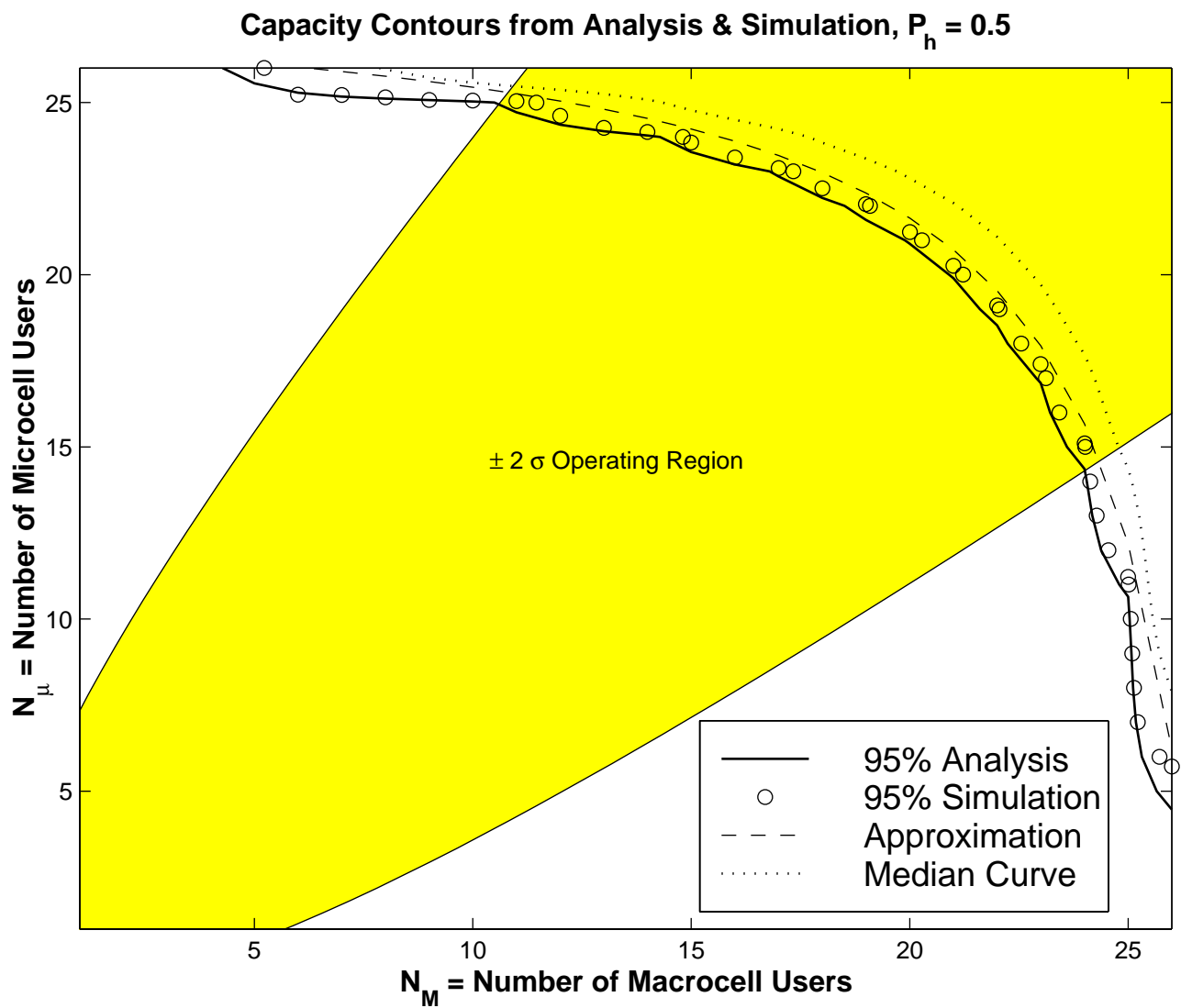


Figure 4: Capacity contours on $N_M - N_\mu$ plane, comparing analysis and simulation results for $P_h = 0.5$ and assuming T-Based selection.

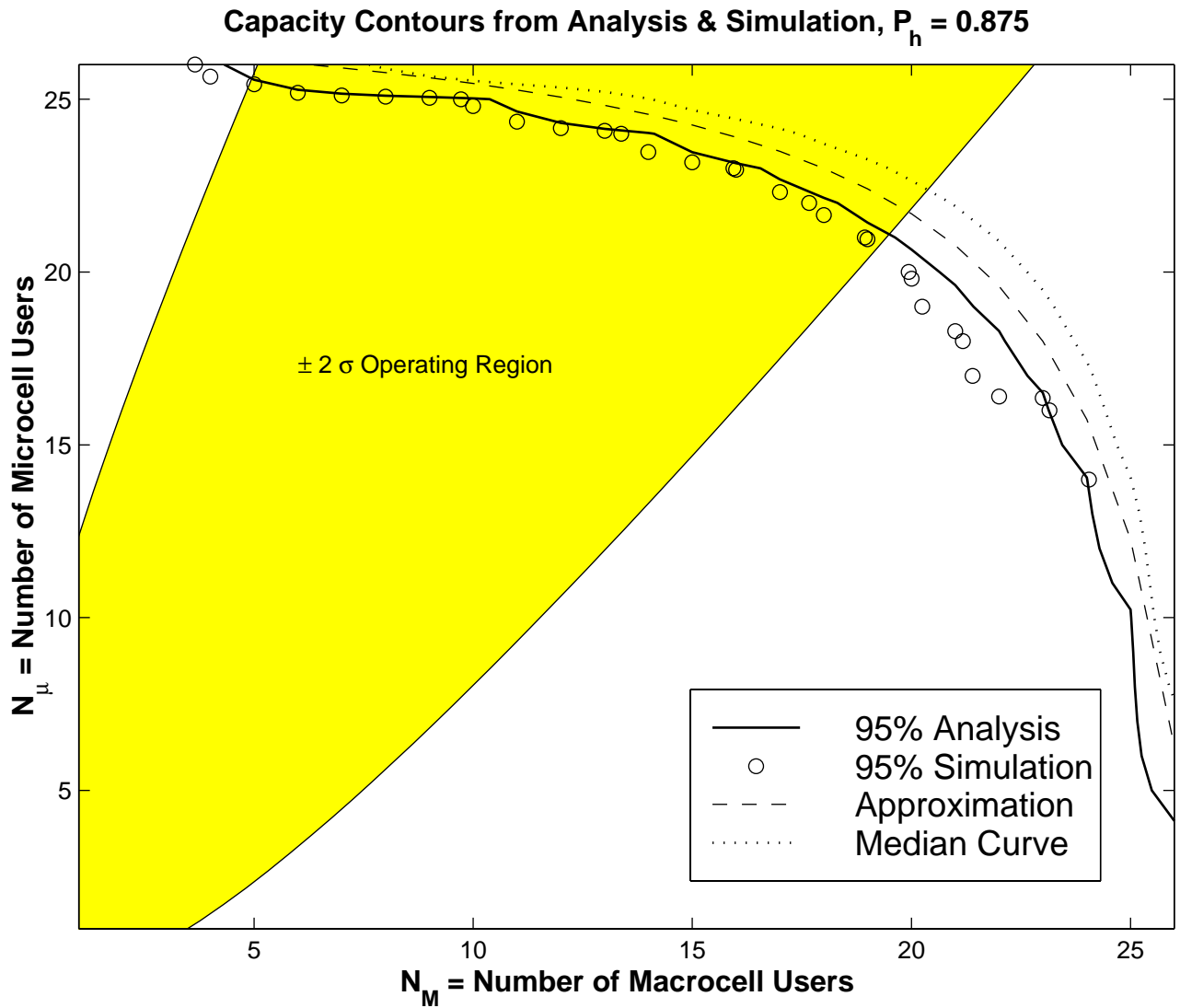


Figure 5: Capacity contours on $N_M - N_\mu$ plane, comparing analysis and simulation results for $P_h = 0.875$ and assuming T-Based selection.

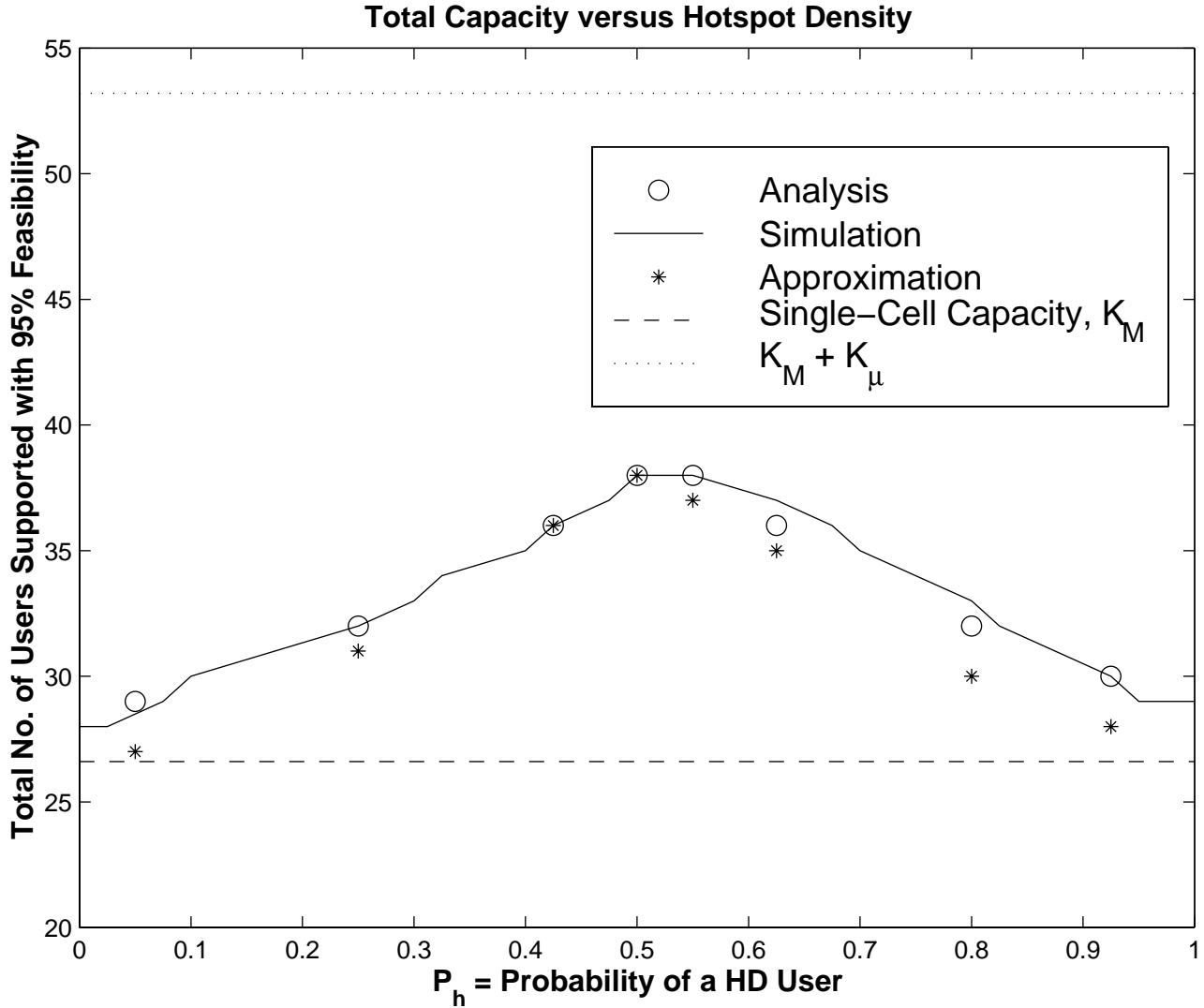


Figure 6: Total capacity, N , versus hotspot density, P_h , comparing analysis and simulation results for T-Based selection. The single-cell capacity is the number of users supported on the uplink in the absence of a microcell. $K_M + K_\mu$ represents the resulting capacity if the system was composed of two non-interfering cells.

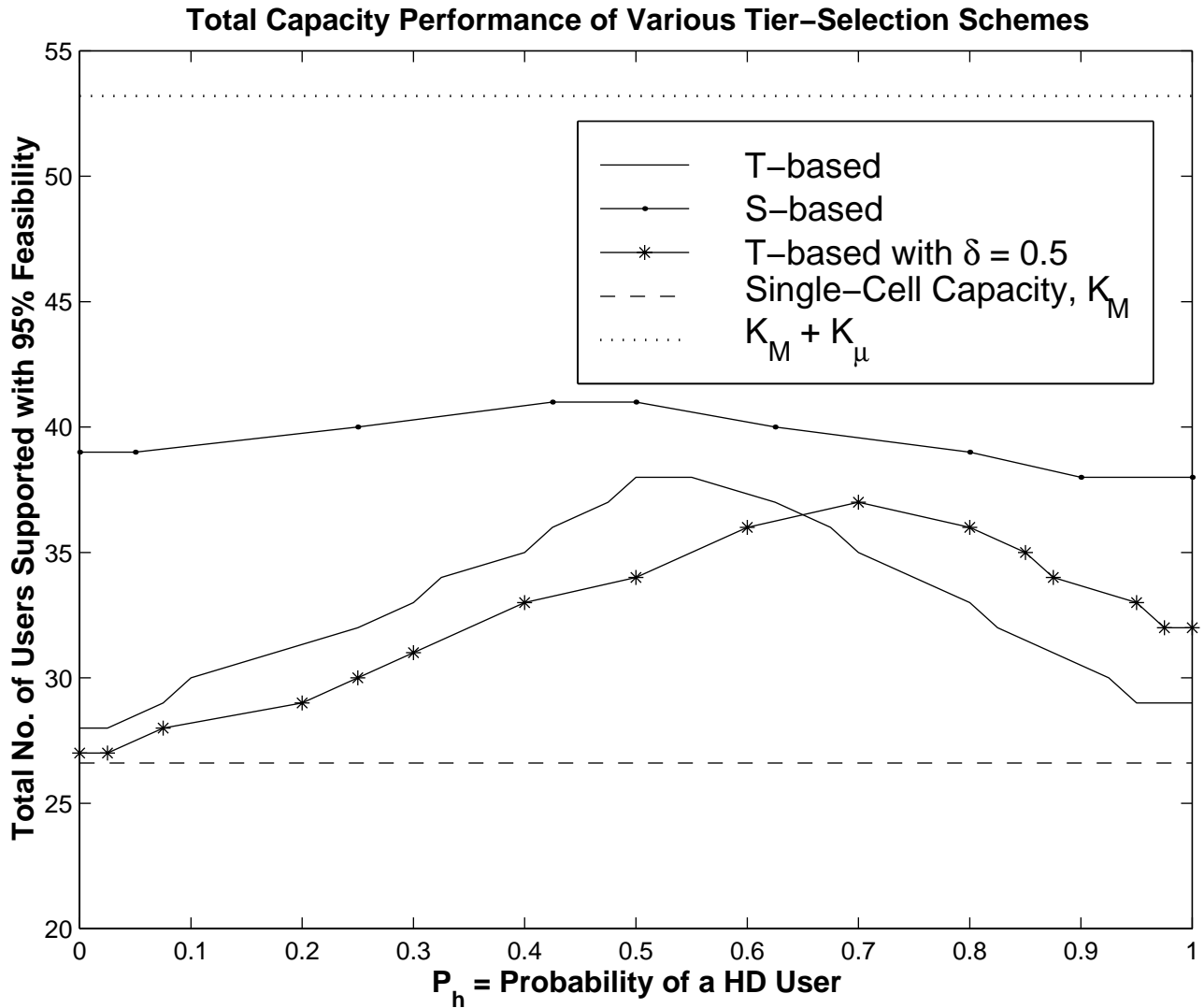


Figure 7: Total capacity, N , versus hotspot density, P_h , for T-Based selection without densensivity, with $\delta = 0.5$, and S-Based selection.

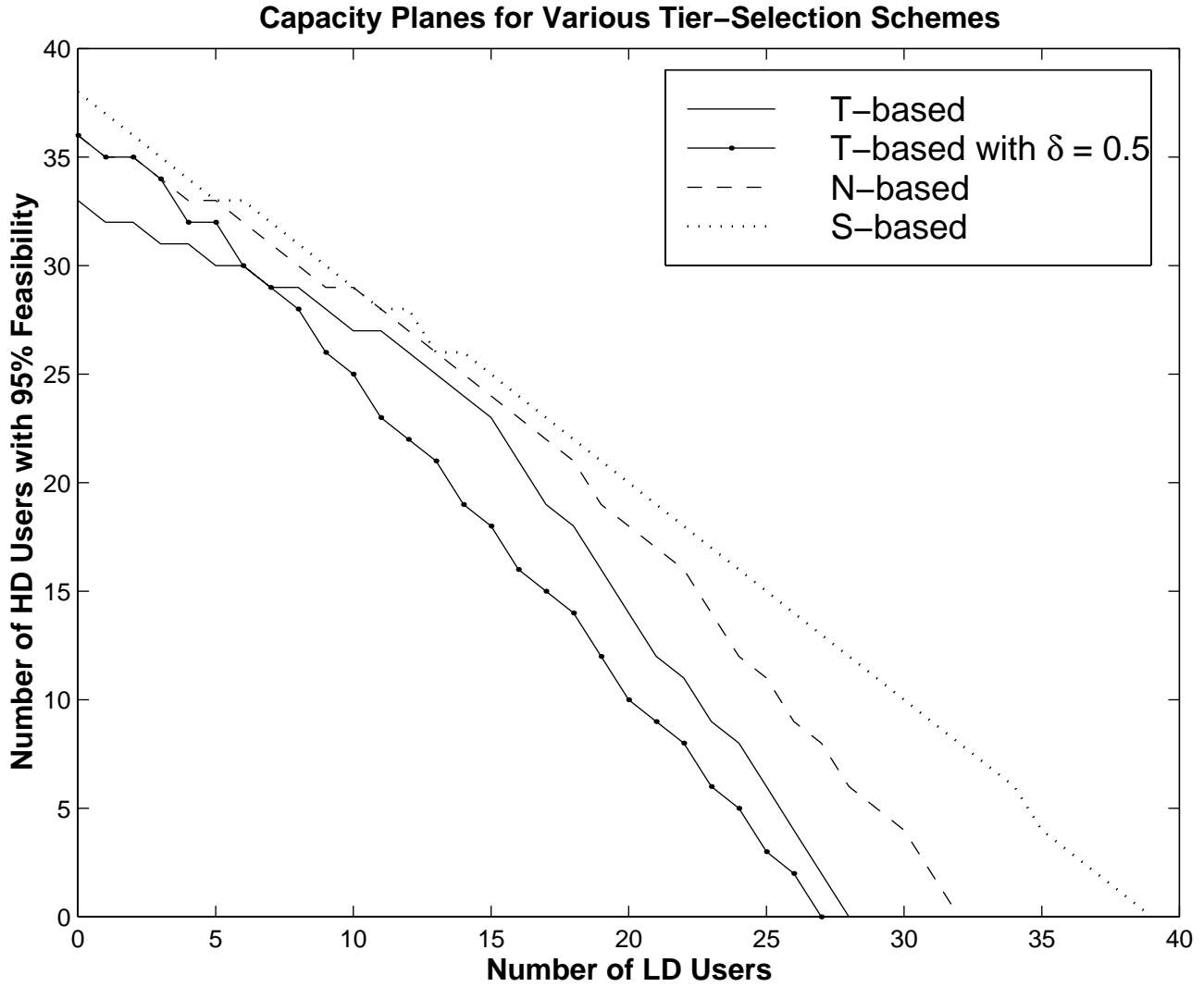


Figure 8: Number of LD users, N_l versus the number of HD users, N_h , supported with feasibility 0.95 for T-Based without desensitivity, with $\delta = 0.5$, N-Based selection, and S-Based selection.